| **Titre:** Title: | Observation of hole injection boost via two parallel paths in Pentacene thin-film transistors by employing Pentacene: 4, 4"-tris(3-methylphenylphenylamino) triphenylamine: MoO₃ buffer layer |
|---|---|
| **Auteurs:** Authors: | Pingrui Yan, Ziyang Liu, Shiming Zhang, Dongyang Liu, Xuehui Wang, Shouzhen Yue, & Yi Zhao |
| **Date:** | 2014 |
| **Type:** | Article de revue / Article |
| **Référence:** Citation: | Yan, P., Liu, Z., Zhang, S., Liu, D., Wang, X., Yue, S., & Zhao, Y. (2014). Observation of hole injection boost via two parallel paths in Pentacene thin-film transistors by employing Pentacene: 4, 4"-tris(3-methylphenylphenylamino) triphenylamine: MoO₃ buffer layer. APL Materials, 2 (11), 116103 (7 pages). https://doi.org/10.1063/1.4901123 |

## Document en libre accès dans PolyPublie
Open Access document in PolyPublie

| **URL de PolyPublie:** PolyPublie URL: | https://publications.polymtl.ca/5180/ |
|---|---|
| **Version:** | Version officielle de l'éditeur / Published version Révisé par les pairs / Refereed |
| **Conditions d'utilisation:** Terms of Use: | CC BY |

## Document publié chez l'éditeur officiel
Document issued by the official publisher

| **Titre de la revue:** Journal Title: | APL Materials (vol. 2, no. 11) |
|---|---|
| **Maison d'édition:** Publisher: | AIP Publishing |
| **URL officiel:** Official URL: | https://doi.org/10.1063/1.4901123 |
| **Mention légale:** Legal notice: | © 2014 Author(s). All article content, except where otherwise noted, is licensed under a Creative Commons Attribution 3.0 Unported License. |

# Observation of hole injection boost via two parallel paths in Pentacene thin-film transistors by employing Pentacene: 4, 4"-tris(3-methylphenylphenylamino) triphenylamine: MoO$_3$ buffer layer

Pingrui Yan, Ziyang Liu, Shiming Zhang, et al.

View Online    Export Citation    CrossMark

## ARTICLES YOU MAY BE INTERESTED IN

Solvent-induced changes in PEDOT:PSS films for organic electrochemical transistors
APL Materials **3**, 014911 (2015); https://doi.org/10.1063/1.4905154

Highly stretchable electrospun conducting polymer nanofibers
Applied Physics Letters **111**, 093701 (2017); https://doi.org/10.1063/1.4997911

Effect of channel thickness, electrolyte ions, and dissolved oxygen on the performance of organic electrochemical transistors
Applied Physics Letters **107**, 053303 (2015); https://doi.org/10.1063/1.4927595
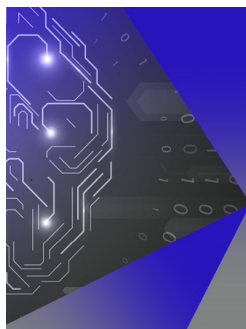
**APL Machine Learning**
Machine Learning for Applied Physics
Applied Physics for Machine Learning
**First Articles Now Online!**

AIP Publishing

# Observation of hole injection boost via two parallel paths in Pentacene thin-film transistors by employing Pentacene: 4,4″-tris(3-methylphenylphenylamino) triphenylamine: MoO$_3$ buffer layer

Pingrui Yan,[1,a] Ziyang Liu,[1,a] Shiming Zhang,[1,2,b] Dongyang Liu,[1] Xuehui Wang,[1] Shouzhen Yue,[1] and Yi Zhao[1,c]

[1]*State Key Laboratory on Integrated Optoelectronics, College of Electronic Science and Engineering, Jilin University, Changchun 130012, People's Republic of China*
[2]*Département of Chemical Engineering, École Polytechnique de Montréal, Montréal, Québec H3C3J7, Canada*

Pentacene organic thin-film transistors (OTFTs) were prepared by introducing 4,4″-tris(3-methylphenylphenylamino) triphenylamine (m-MTDATA): MoO$_3$, Pentacene: MoO$_3$, and Pentacene: m-MTDATA: MoO$_3$ as buffer layers. These OTFTs all showed significant performance improvement comparing to the reference device. Significantly, we observe that the device employing Pentacene: m-MTDATA: MoO$_3$ buffer layer can both take advantage of charge transfer complexes formed in the m-MTDATA: MoO$_3$ device and suitable energy level alignment existed in the Pentacene: MoO$_3$ device. These two parallel paths led to a high mobility, low threshold voltage, and contact resistance of 0.72 cm$^2$/V s, −13.4 V, and 0.83 kΩ at V$_{ds}$ = −100 V. This work enriches the understanding of MoO$_3$ doped organic materials for applications in OTFTs. © 2014 Author(s). All article content, except where otherwise noted, is licensed under a Creative Commons Attribution 3.0 Unported License. [http://dx.doi.org/10.1063/1.4901123]

Organic electronics has revolutionized the way we generate, manipulate, and display information. Organic light-emitting diodes (OLEDs),[1–3] one of the forerunners of organic electronics, have already been commercially produced in real market for cell phones, digital cameras, and automotive electronics. Flexible electrophoretic displays and portable organic solar cells (OSCs) are highly praised due to their potential to solve the energy and environmental issues in the near future.[4] The past few years have seen the significant progress in the research of organic thin-film transistors (OTFTs), which has special advantages to provide low-cost, flexible, and easy to make devices as compared to inorganic thin film transistors and complementary metal oxide semiconductor technology.[5–8] However, despite tremendous effort has been devoted to develop suitable device architectures or efficient materials in order to satisfy potential commercial requirements for OTFTs, this technology still poses a big challenge in practice due to the lower carrier mobility as well as higher threshold voltage (V$_{th}$) compared to inorganic competitors. Among these organic materials being ever used in demonstrating OTFTs, Pentacene-based devices are more attractive due to their preferable comprehensive features, such as relatively higher field-effect mobility, lower V$_{th}$, and higher saturation current.[9] Unluckily, the direct contact between metal electrodes and Pentacene induces metallic mixture and dipoles at the interface, which subsequently increases the interface resistance and results in an unexpected degradation of the device performance.[10,11] This critical issue could be

---

[a]P. Yan and Z. Liu contributed equally to this work.
[b]Electronic mail: zhangshimingjlu@gmail.com.
[c]Author to whom correspondence should be addressed. Electronic mail: yizhao@jlu.edu.cn.

relieved with the introduction of a buffer layer between the electrodes and the Pentacene. Up to now, lots of work have been dedicated in an effort to optimize the performance of OTFTs by seeking ideal buffer layers.[7,12,13]

Metal oxides, such as $MoO_3$,[14] $V_2O_5$,[8] and $WO_3$,[15] have already been introduced as buffer layers for OLEDs, OSCs, as well as OTFTs. In particular, the past few years have seen the rise of $MoO_3$ study as buffer layers in OTFTs.[16,17] Electrical doping of $MoO_3$ into organic materials as buffer layers has also been proved to be an efficient way to improve the device performance.[6] For Pentacene based OTFTs, the organic materials employed for the buffer layer should be highly conductive for holes. One of the most promising P-type materials is 4, 4″-tris(3-methylphenylphenylamino) triphenylamine (m-MTDATA), which has been widely adopted to demonstrate high efficiency OLEDs. In 2011, m-MTDATA was first introduced as buffer layer to OTFTs by Jiang *et al.*[7] In 2013, Su *et al.* doped $V_2O_5$ into m-MTDATA, and the performance was largely improved.[8] They all ascribed the performance improvement of the OTFTs to the weakening of the interface dipole and the lowering of the energy barrier after employing m-MTDATA or m-MTDATA: $V_2O_5$ as buffer layers.

In 2008, our group had doped $MoO_3$ into m-MTDATA to act as an enhanced hole injection layer in OLEDs by making use of the formation of charge transfer complexes (CTC) and we reported that this strategy can significantly decrease the turn-on voltage to 2.35 V, which is close to the thermodynamic limit of tris (8-hydroxy-quinolinato) aluminium ($Alq_3$)-based green OLEDs.[18] In this work, we investigate the role of m-MTDATA: $MoO_3$, Pentacene: $MoO_3$, and Pentacene: m-MTDATA: $MoO_3$ as buffer layers in the bottom gate OTFTs based on polymethylmethacrylate (PMMA) insulator. The hole mobility of the Pentacene: m-MTDATA: $MoO_3$ device is significantly increased up to 0.72 $cm^2$/V s, which is 5 times higher than the reference device (0.14 $cm^2$/V s). Moreover, the $V_{th}$ drops from $-42.9$ V to $-13.4$ V ($V_g = -100$ V). These performances are superior to all other compared devices based on m-MTDATA, Pentacene: $MoO_3$, and m-MTDATA: $MoO_3$ buffer layers presented here. This work reveals that the better energy level alignment, together with CTC formed in Pentacene: m-MTDATA: $MoO_3$ system, co-contributes to the boost of hole density, resulting in a conductivity enhancement and thereby improved device performance.

The schematic structure of Pentacene OTFT fabricated in this study is shown in Fig. 1. PMMA was dissolved in n-Butyl acetate solvent with a concentration of 11 wt. %. The solution was then spin-coated on the indium tin oxide (ITO) glass substrate at a rate of 3000 rpm for 30 s and dried on a hotplate at 120 °C for 2 h under ambient atmosphere. A dielectric film with a thickness of 1150 nm and capacitance of 1.7 $nF/cm^2$ was finally obtained. Pentacene (30 nm) and the buffer layer (10 nm) were thermally deposited in vacuum ($\sim$4.0 $\times$ 10$^{-4}$ Pa) at a rate of 0.5-1 Å/s monitored *in situ* with the quartz oscillator. The Pentacene, m-MTDATA, and $MoO_3$ buffer layers were co-evaporated in different boats. Subsequently, the samples were transferred to the metal chamber for
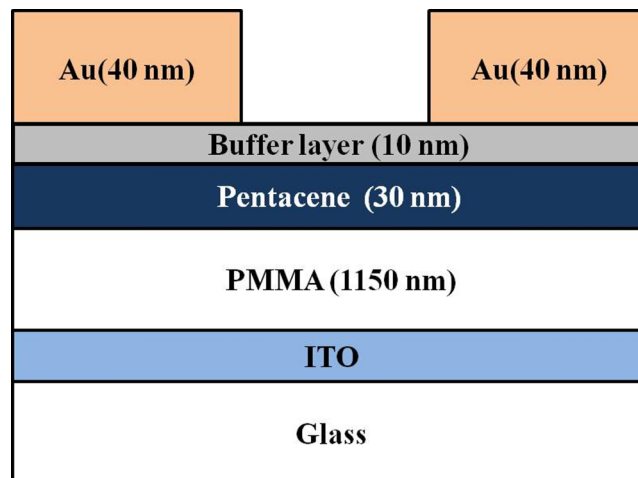


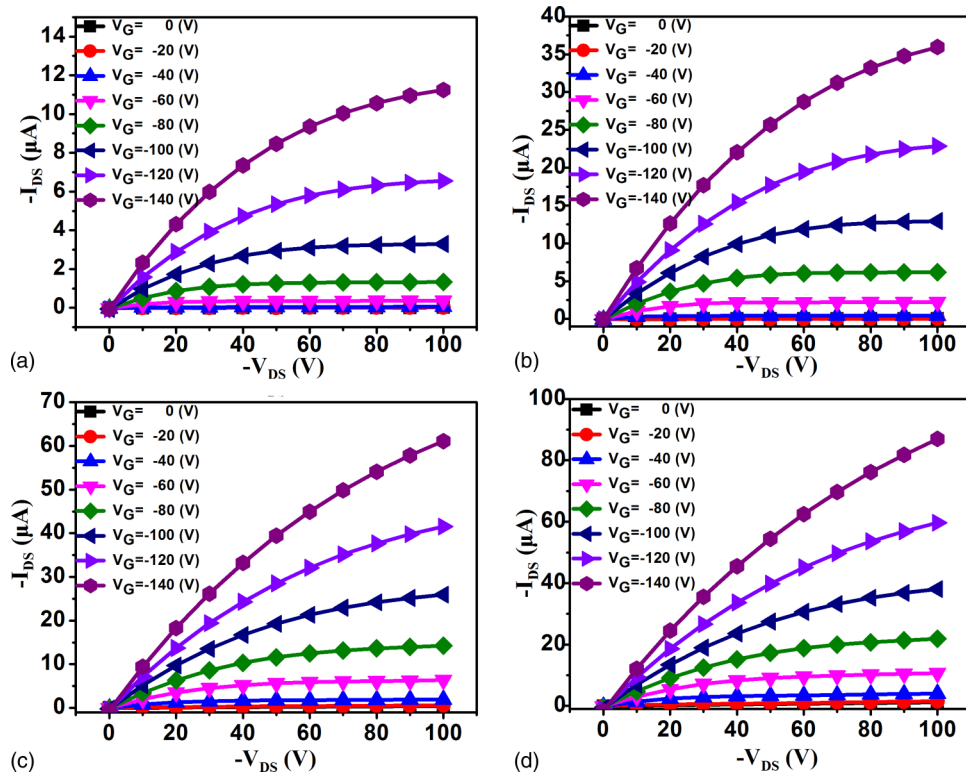FIG. 1. Device structure of OTFTs studied in this work.

FIG. 2. Output characteristics of devices based on a buffer layer of (a) pure Pentacene, (b) Pentacene: $MoO_3$, (c) m-MTDATA: $MoO_3$, and (d) Pentacene: m-MTDATA: $MoO_3$.

depositing 40 nm Au source-drain electrodes and suffered from a vacuum break due to the change of the shadow mask. The channel width (W) and length (L) are 1000 $\mu$m and 100 $\mu$m, respectively. Atomic force microscopy (AFM) measurement was carried out on Veeco-3100. The absorption (Abs.) spectrum was measured by means of ultraviolet/visible spectrometer (UV 3600, Shimadzu). The electrical characteristics of the OTFTs were measured with two combined Keithley 2400 programmable voltage-current sources in atmosphere at room temperature.

The transfer and output characteristics of our devices are shown in Fig. S1 (supplementary material[19]) and Fig. 2, respectively. OTFTs with different buffer layers are compared to reference OTFTs having the same geometry. All these devices exhibited typical p-channel characteristics. From the output curves in the saturation regime ($V_{ds} = -100$ V), we extracted the best value of effective mobility ($\mu_{eff}$) $\approx 0.72$ cm$^2$/V s and $V_{th} \approx -13.4$ V for Pentacene: m-MTDATA: $MoO_3$ device and the worst value of $\mu_{eff} \approx 0.14$ cm$^2$/V s and $V_{th} \approx -42.9$ V for the reference device. The values of the Pentacene: m-MTDATA: $MoO_3$ device are close to those of state-of-the-art Pentacene OTFTs obtained on PMMA insulator at higher $V_g$. The detailed performances of the OTFTs studied in this work are summarized in Table I. Total resistances ($R_{total}$) of the devices shown in Table I were estimated utilizing the method presented by Yagi *et al.*[20]

Fig. 3(a) shows the $I_{ds}$ vs $V_{ds}$ curves in OTFTs with different buffer layers at a fixed gate voltage of $-100$ V. As illustrated, the drain current ($V_{ds} = -100$ V) in the Pentacene: $MoO_3$ device (12.93 $\mu$A) is four times higher than the reference device (3.29 $\mu$A) and that of the m-MTDATA: $MoO_3$ device (25.91 $\mu$A) is eight times higher than the reference. In particular, $I_{ds}$ of the device based on Pentacene: m-MTDATA: $MoO_3$ buffer layer outperforms all other compared devices and the $I_{ds}$ increases up to 38.05 $\mu$A, which is almost 12 times higher than the reference device. According to our previous study,[18] one of the main reasons for the $I_{ds}$ increase in m-MTDATA: $MoO_3$ device can be ascribed to the CTC formed in the buffer layer, which can largely increase the hole density between Au and Pentacene, resulting in enhanced conductivity of Pentacene channel layer. However,

TABLE I. Detailed summaries of devices studied in this work based on buffer layers of (a) pure Pentacene, (b) Pentacene: $MoO_3$ (1: 0.1), (c) m-MTDATA: $MoO_3$ (1: 0.1), (d) Pentacene: m-MTDATA: $MoO_3$ (0.5: 0.5: 0.1), and (e) pure m-MTDATA (also as a reference device here).

| Device | a | b | c | d | e |
|---|---|---|---|---|---|
| $\mu_{eff}$ (cm$^2$/V s)[a] | 0.14 | 0.36 | 0.40 | 0.72 | 0.15 |
| $V_{th}$ (V)[a] | −42.9 | −33.7 | −20.7 | −13.4 | −42 |
| $g_m$ (S)[a] | $2.38 \times 10^{-7}$ | $6.12 \times 10^{-7}$ | $6.8 \times 10^{-7}$ | $1.2 \times 10^{-6}$ | $2.55 \times 10^{-7}$ |
| $R_{total}$ (k$\Omega$)[b] | 5.90 | 1.92 | 1.25 | 0.83 | 5.00 |

[a]The values of $\mu_{eff}$, $V_{th}$, and transconductance ($g_m$) were calculated at saturation region ($V_{ds} = -100$ V).
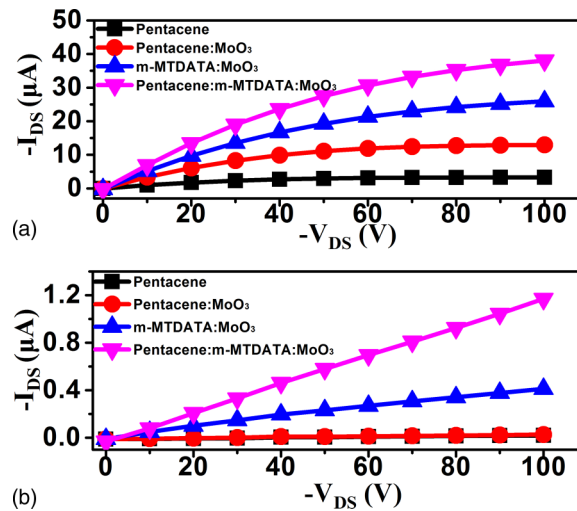[b]$R_{total}$ was calculated at $V_g = -140$ V.



FIG. 3. $I_{ds}$ versus $V_{ds}$ curves of devices based on different buffer layers at a gate voltage of (a) −100 V and (b) 0 V.

the CTC is not supposed to be formed in the Pentacene: $MoO_3$ film because no additional broad absorption is observed over the entire spectra-scan region by comparing the Abs. spectra of pure Pentacene and Pentacene: $MoO_3$ samples (Fig. 4). This is further confirmed by the output character of the devices operated at $V_g = 0$ V. In the absence of the gate voltage, $I_{ds}$ profiles for our devices can directly describe the hole density in the buffer layers, since the $I_{ds}$ is dominated by the conductivity of the buffer layer rather than the Pentacene channel layer. As shown in Fig. 3(b), $I_{ds}$ of m-MTDATA: $MoO_3$ device is obviously higher than the Pentacene reference device due to the hole density increase caused by CTC in the m-MTDATA: $MoO_3$ system, while the plots for Pentacene and Pentacene: $MoO_3$ devices are virtually identical ($I_{ds} \approx 0$ $\mu$A). This is a direct evidence which demonstrates that doping of $MoO_3$ into Pentacene under thermal evaporation condition has almost no effect on its hole density. In this case, the $I_{ds}$ increases for the Pentacene: $MoO_3$ device at $V_g = -100$ V, where $I_{ds}$ is dominated by the field-induced holes in Pentacene channel layer, should be other mechanisms rather than the CTC formation in the Pentacene: $MoO_3$ buffer layer. The results are consistent with the conclusion proposed by Wang *et al.*, who ascribed the performance improvement of the Pentacene: $MoO_3$ device to the offset drops between the highest occupied molecular orbital (HOMO) and Fermi energy level ($E_F$) of Pentacene.[6] They also assumed that CTC may exist in the Pentacene: $MoO_3$ system, while our observations exclude this possibility, and we recognize that the suitable energy level alignment should be responsible for the $I_{ds}$ increase at $V_g = -100$ V.

The above discussions expose the underlying reason for the impressive performance improvement of our Pentacene: m-MTDATA: $MoO_3$ device: $I_{ds}$ is superior to all other competitors, the value at $V_g = -100$ V, Vds $= -100$ V is even 1.5 times higher than the m-MTDATA: $MoO_3$ device (see Fig. 3(a)). Having taken into consideration of the above analysis, along with comparison to previous works on different buffer layers,[6–8,16] we conclude herein the key point of this work,
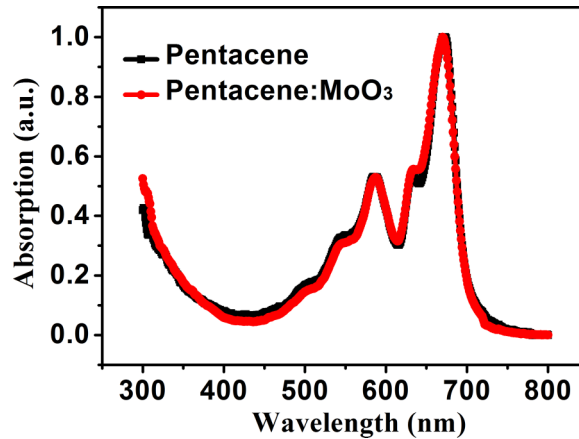
FIG. 4. Abs. spectra of pure Pentacene and Pentacene: $MoO_3$ (1: 0.1) films with a structure of quartz substrate/X (30 nm). X stands for Pentacene and Pentacene: $MoO_3$, respectively.

i.e., the Pentacene: m-MTDATA: $MoO_3$ device presented here has realized the unique potential to take advantage of both the CTC formed in the m-MTDATA: $MoO_3$ device and the suitable band banding existed in the Pentacene: $MoO_3$ device. That is, the Pentacene: m-MTDATA: $MoO_3$ device not only increases the hole density between the Au electrode and the Pentacene due to the CTC formed in m-MTDATA: $MoO_3$ components (see Fig. S2 in the supplementary material[19]) but also achieves better energy level aligning of the Au work function with the HOMO level of Pentacene, that is similar to the Pentacene: $MoO_3$ system (Fig. 5).[6] These two parallel paths together boost the hole injection to the Pentacene layer and thereby contribute to the high $\mu_{eff}$, low $V_{th}$, and $R_{total}$ of the Pentacene: m-MTDATA: $MoO_3$ device (Table I). One can also note that $I_{ds}$ of the Pentacene: m-MTDATA: $MoO_3$ device at $V_g = 0$ V is the highest among the compared devices, again a clear signifier of the above conclusion. However, it should be mentioned that although the Pentacene: m-MTDATA: $MoO_3$ is proved to be an advanced buffer layer over the other candidates, the $I_{on}/I_{off}$ ratio of the Pentacene: m-MTDATA: $MoO_3$ device presented here actually is not high (on the level of $\sim 10^2$). This is because, the device has a leakage current via the buffer layer at $V_g = 0$ V (higher $I_{off}$) and the buffer layer has no field-effect (see Fig. S3 in the supplementary material[19]). The $I_{on}/I_{off}$ ratio issue is expected to be solved by either evaporating the buffer layer and Au electrodes by sequence with the same shadow mask or patterning the buffer layer using orthogonal photoresist.[21]

AFM characterization is further implemented since the device performance may also be affected by the morphology of the buffer layers. As shown in Fig. 6, the root-mean-square (rms) roughness of Pentacene: m-MTDATA: $MoO_3$ film is decreased to 3.21 nm compared with 4.33 nm in pure Pentacene reference film, which is also better than the Pentacene: $MoO_3$ device ($\sim 3.68$ nm).[6] The
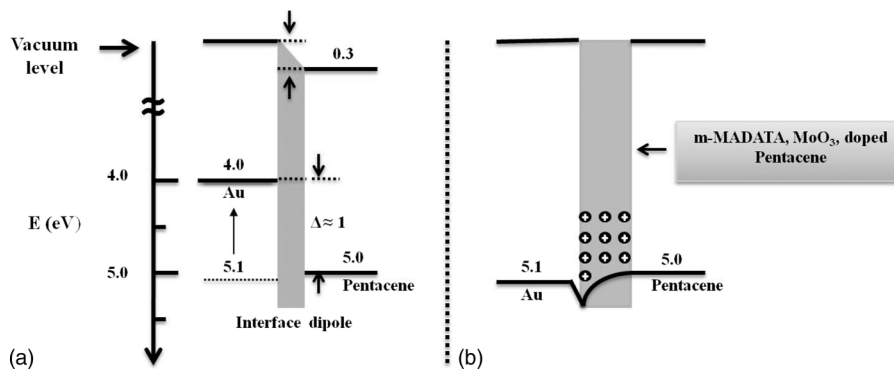


FIG. 5. Energy level sketch for devices (a) without buffer layer[9,10] and (b) with Pentacene: m-MTDATA: $MoO_3$ buffer layer.
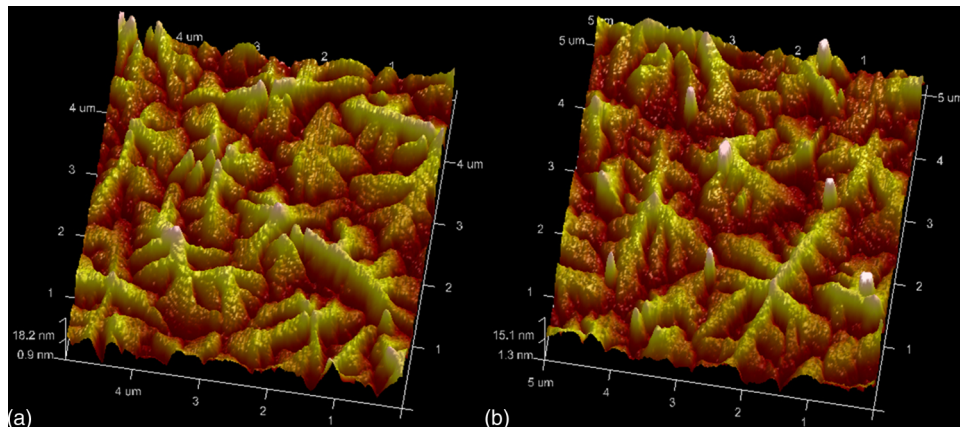
FIG. 6. AFM images of surface morphologies of (a) pure Pentacene film (40 nm) and (b) Pentacene: m-MTDATA: $MoO_3$ film (0.5: 0.5: 0.1, 10 nm) on Pentacene film (30 nm). Rms roughness is 4.33 nm for the former film and 3.21 nm for the latter film, respectively.

more smooth film morphology of Pentacene: m-MTDATA: $MoO_3$ film can realize better contact and may be one of the reasons for the suitable energy level alignment between Au and Pentacene because the surface roughness decrease is helpful to lower the barrier height.[22]

Fig. 7 shows the J-V curves of hole-only devices for characterizing the hole injection capacity directly into ITO which is a standard electrode in the traditional OLEDs architecture. Compared with the current density of the m-MTDATA: $MoO_3$ ($6.6 \times 10^3 \mu A$) that is commonly used for demonstrating efficient OLEDs (especially for lower turn-on voltage),[18,23] the current density of Pentacene: m-MTDATA: $MoO_3$ device reaches up to $9.1 \times 10^3$ $\mu A$ at 10 V. Therefore, it is believed that the Pentacene: m-MTDATA: $MoO_3$ strategy developed in this work may have great potential application to enhance the hole injection for OLEDs as well as other organic electronics devices in the future. More details about this work will be presented later, and the performance is expected to be largely improved after optimization.

In summary, we have demonstrated Pentacene thin-film transistors employing Pentacene: m-MTDATA: $MoO_3$ as buffer layer. The device can take advantage of both the CTC in the m-MTDATA: $MoO_3$ system and suitable energy level alignment in the Pentacene: $MoO_3$ system. As a result, the $\mu_{eff}$ was significantly increased from 0.14 $cm^2$/V s to 0.72 $cm^2$/V s and $V_{th}$ was lowered from $-42.9$ V to $-13.4$ V, respectively, as compared to the reference device. AFM characterization
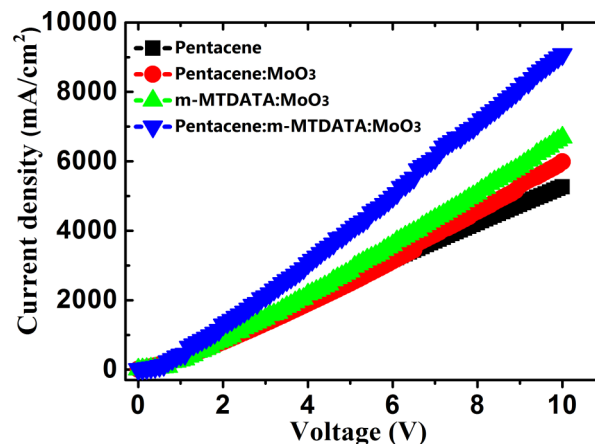


FIG. 7. Current density (J) versus voltage plots of devices based on different hole injection layers with detailed structure of ITO/hole injection layers (40 nm)/Au (40 nm).

shows that the surface morphology was also greatly ameliorated. It is anticipated that this strategy can be applicable to other organic electronics devices, and this work might inspire new ideals towards more efficient hole injection buffer layers for high performance OTFTs.

[1] S. Reineke, F. Lindner, G. Schwartz, N. Seidler, K. Walzer, B. Lüssem, and K. Leo, Nature **459**(7244), 234–238 (2009).

[2] S. Zhang, S. Yue, Q. Wu, Z. Zhang, Y. Chen, X. Wang, Z. Liu, G. Xie, Q. Xue, and D. Qu, Org. Electron. **14**(8), 2014–2022 (2013).

[3] Q. Xue, S. Zhang, G. Xie, Z. Zhang, L. Zhao, Y. Luo, P. Chen, Y. Zhao, and S. Liu, Solid-State Electron. **57**(1), 35–38 (2011).

[4] B. Kippelen and J.-L. Brédas, Energy Environ. Sci. **2**(3), 251–261 (2009).

[5] C. D. Dimitrakopoulos and D. J. Mascaro, IBM J. Res. Dev. **45**(1), 11–27 (2001).

[6] Z. Wang, M. W. Alam, Y. Lou, S. Naka, and H. Okada, Appl. Phys. Lett. **100**(4), 043302 (2012).

[7] X. Yu, J. Yu, J. Zhou, J. Huang, and Y. Jiang, Appl. Phys. Lett. **99**(6), 063306 (2011).

[8] S.-H. Su, C.-M. Wu, S.-Y. Kung, and M. Yokoyama, Thin Solid Films **536**, 229–234 (2013).

[9] J. Lee, K. Kim, J. H. Kim, S. Im, and D.-Y. Jung, Appl. Phys. Lett. **82**(23), 4169–4171 (2003).

[10] F.-C. Chen, L.-J. Kung, T.-H. Chen, and Y.-S. Lin, Appl. Phys. Lett. **90**(7), 073504 (2007).

[11] N. Watkins, L. Yan, and Y. Gao, Appl. Phys. Lett. **80**(23), 4384–4386 (2002).

[12] J. Seo, D. Park, S. Cho, C. Kim, W. Jang, C. Whang, K.-H. Yoo, G. Chang, T. Pedersen, and A. Moewes, Appl. Phys. Lett. **89**(16), 163505 (2006).

[13] X. Qian, T. Wang, and D. Yan, Appl. Phys. Lett. **103**(17), 173512 (2013).

[14] H. You, Y. Dai, Z. Zhang, and D. Ma, J. Appl. Phys. **101**(2), 026105 (2007).

[15] J. Li, X.-W. Zhang, L. Zhang, K.-u. Haq, X.-Y. Jiang, W.-Q. Zhu, and Z.-L. Zhang, Semicond. Sci. Technol. **24**(11), 115012 (2009).

[16] C.-W. Chu, S.-H. Li, C.-W. Chen, V. Shrotriya, and Y. Yang, Appl. Phys. Lett. **87**(19), 193508 (2005).

[17] Y. Guo, Y. Liu, C.-a. Di, G. Yu, W. Wu, S. Ye, Y. Wang, X. Xu, and Y. Sun, Appl. Phys. Lett. **91**(26), 263502 (2007).

[18] G. Xie, Y. Meng, F. Wu, C. Tao, D. Zhang, M. Liu, Q. Xue, W. Chen, and Y. Zhao, Appl. Phys. Lett. **92**(9), 093305 (2008).

[19] See supplementary material at http://dx.doi.org/10.1063/1.4901123 for transfer curves of transistors, Abs spectrum and field-effect behavior of Pentacene: m-MTDATA: MoO$_3$ film.

[20] I. Yagi, K. Tsukagoshi, and Y. Aoyagi, Appl. Phys. Lett. **84**(5), 813–815 (2004).

[21] P. G. Taylor, J.-K. Lee, A. A. Zakhidov, M. Chatzichristidi, H. H. Fong, J. A. DeFranco, G. G. Malliaras, and C. K. Ober, Adv. Mater. **21**(22), 2314–2317 (2009).

[22] C. Bock, D. Pham, U. Kunze, D. Kafer, G. Witte, and C. Woll, J. Appl. Phys. **100**(11), 114517 (2006).

[23] Z. Zhang, G. Xie, S. Yue, Q. Wu, Y. Chen, S. Zhang, L. Zhao, Y. Luo, Y. Zhao, and S. Liu, Org. Electron. **13**(11), 2296–2300 (2012).